AGU PUBLICATIONS

Geochemistry, Geophysics, Geosystems

RESEARCH ARTICLE
10.1002/2013GC005124

**Key Points:**
- There is a highly variable lithospheric structure throughout the Gibraltar Arc
- Slab is delaminating continental lithosphere in Gibraltar Arc
- Slab pull force is exerted on base of lithosphere causing depression of Moho

**Supporting Information:**
- AuxiliaryMaterialREADME.
- AuxiliaryMaterial_Figure 1–8

**Correspondence to:**
S. Thurner,
smt4@rice.edu

**Citation:**
Thurner, S., I. Palomeras, A. Levander, R. Carbonell, and C.-T. Lee (2014), Ongoing lithospheric removal in the western Mediterranean: Evidence from Ps receiver functions and thermobarometry of Neogene basalts (PICASSO project), *Geochem. Geophys. Geosyst.*, *15*, 1113–1127, doi:10.1002/2013GC005124.

Received 30 OCT 2013
Accepted 28 FEB 2014
Accepted article online 6 MAR 2014
Published online 22 APR 2014

# Ongoing lithospheric removal in the western Mediterranean: Evidence from Ps receiver functions and thermobarometry of Neogene basalts (PICASSO project)

**Sally Thurner[1], Imma Palomeras[1], Alan Levander[1], Ramon Carbonell[2], and Cin-Ty Lee[1]**

[1]Department of Earth Science, Rice University, Houston, Texas, USA, [2]Department of Structure and Dynamics of the Earth, CSIC—Institute of Earth Science Jaume Almera, Barcelona, Spain

**Abstract** The western Mediterranean tectonic system consists of the Betic Mountains in southern Spain and the Rif Mountains in northern Morocco curved around the back-arc extensional Alboran basin. Multiple tectonic models have been developed to explain the coeval compressional and extensional tectonic processes that have affected the western Mediterranean since the Oligocene. In order to provide constraints on these evolutionary models, we use Ps teleseismic receiver functions (RF), thermobarometric analyses of post-Oligocene basalts, and previous teleseismic tomography images to investigate the lithospheric structure of the region. Ps RFs were calculated using seismic data from 239 broadband seismic stations in southern Iberia and northern Morocco and thermobarometric analysis was performed on 19 volcanic samples distributed throughout the region. The RF images reveal a highly variable Moho depth (~25 to ~55 km), as well as a strong positive, sub-Moho horizon between ~45 and ~80 km depth beneath the central Betic and Rif Mountains, which we interpret to be the top of the previously imaged Alboran Sea slab. Thermobarometric constraints from magmas in the eastern Betics and Rif indicate mantle melting depths between 40 and 60 km, typical of melting depths beneath mid-oceanic ridges where little to no lithosphere exists. Together, the RF and thermobarometric data suggest ongoing and recent slab detachment resulting from delamination of the continental lithosphere.

## 1. Introduction

The Africa-Eurasia collision has resulted in a diffuse deformation zone within and around the Mediterranean Sea, where multiple narrow arcs and back-arc extensional basins have formed since the Oligocene [*Rosenbaum*, 2002]. The western Mediterranean, comprising the westernmost range of the Alpine-Himalayan system, includes the Betic and Rif orogens curved around the Alboran back-arc extensional basin (Figure 1a). Beginning in the Miocene, the region extending from the Betic Mountains in southern Spain to the Atlas Mountains in Morocco, has been affected not only by collisional processes resulting from Africa-Eurasia convergence, but also by extensional processes initiated by slab rollback [*Royden*, 1993; *Lonergan* and *White*, 1997; *Rosenbaum*, 2002]. Multiple continental lithospheric removal events have also been proposed to explain the extension that has occurred throughout region [*Platt and Vissers*, 1989; *Duggen et al*., 2005]. Additionally, the western Mediterranean has been affected by widespread volcanism. The region is marked by a ~300 km northeast-southwest trending corridor of Miocene to Pleistocene igneous activity. This corridor extends from Spain through the Alboran Sea and into Morocco (Figure 1a) [*Duggen et al*., 2004]. The spatial and temporal variability of volcanic rocks found within this corridor suggests a transition from post-collisional subduction related magmatism to intraplate magmatism [*Duggen et al*., 2005].

Although multiple geodynamic models have been proposed to explain western Mediterranean tectonics and volcanic activity, a consensus has not been reached thus far. With a view toward better understanding the complex geodynamics of the Alboran system, several temporary and permanent broadband seismic arrays have been deployed. Together, the PICASSO array (Program to Investigate Convective Alboran Sea System Overturn), the IberArray, the Portuguese National Seismograph Network, the Spanish Digital Seismic Network, the University of Lisbon Seismic Network, and the Western Mediterranean Seismic Network provide dense broadband station coverage of southern Iberia and Morocco (Figure 1b). Using data from a total of 239 broadband seismic stations and 19 volcanic samples, we present a teleseismic Ps (*P* wave to *S* wave) receiver function (RF) and thermobarometric analysis of the western Mediterranean. The goal of this

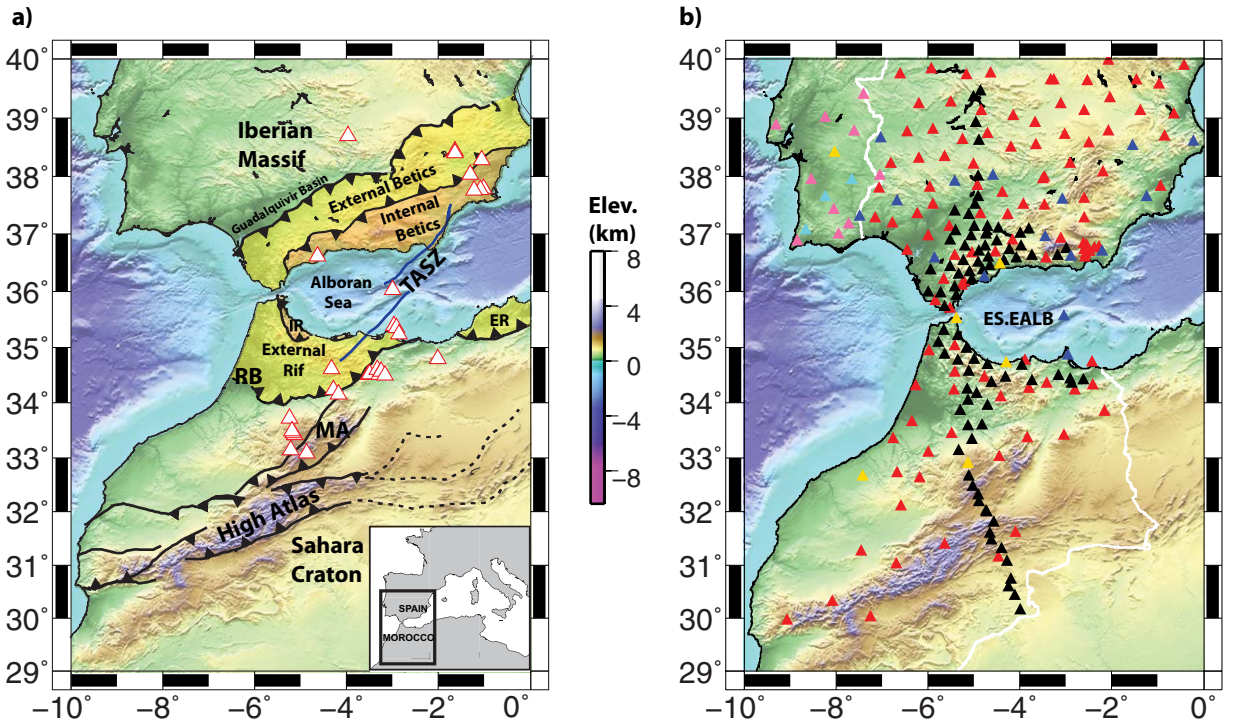


| Network | Number of Stations |
|---|---|
| IberArray (IB) | 110 |
| PICASSO Network (XB) | 85 |
| Portuguese National Sesimograph Network (PM) | 10 |
| Spanish Digital Seismic Network (ES) | 26 |
| University of Lisbon Seismic Network (LX) | 3 |
| Western Mediterranean Seismic Network (WM) | 6 |

External Betic-Rif Arc
Internal Betic-Rif Arc
Left-slip fault
Thrust fault
Cenozoic volcanic field
**TASZ** - Tran-Alboran Shear Zone
**ER** - External Rif Mountains
**IR** - Internal Rif Mountains
**RB** - Rharb Basin
**MA** - Middle Atlas Mountains

**Figure 1.** (a) Map showing the elevation and major geologic features in the western Mediterranean. (b) Map showing the locations of the 239 stations used in this study.

research is to provide crustal and upper mantle constraints on the evolutionary tectonic models that have been proposed for this region. Our analysis, interpreted in conjunction with previous teleseismic tomography images, provides evidence for ongoing lithospheric delamination, initiated by slab rollback and vertical slab-pull forces acting on the base of the Gibraltar Arc continental lithosphere.

## 2. Tectonic Framework

The Gibraltar Arc, consisting of the Betic and Rif mountain systems, formed as the result of a series of tectonic events beginning with Africa-Iberia convergence ~50 Ma. At this time, units along the eastern Iberian margin were stacked to form the Alboran Domain with continental crust thickened to ~50–60 km [*Vissers et al.*, 1995]. Around 35 Ma, a northwest dipping subduction system developed along the southeastern margin of Iberia [*Rosenbaum*, 2002] where rapid slab rollback to the southeast was initiated by the gravitational instability of old (>110 Ma) subducting lithosphere and/or the slowing of Africa-Eurasia convergence [*Rosenbaum*, 2002]. Slab rollback resulted in significant extension within the Alboran Domain, the transport of the Alboran Domain southwestward across the Mediterranean, and the development of an eastward

dipping subduction system between Iberia and Africa. Fragments of the westward migrating Alboran continental crust were eventually thrust onto the passive margins of Africa and Iberia, forming the Betic and Rif orogens [*Rosenbaum*, 2002]. These orogens now consist of External Domains, consisting of shortened passive continental margin rocks, and Internal Domains, consisting of the previously deformed Paleozoic to Early Miocene Alboran rocks that were thrust onto the two continental margins (Figure 1a) [*Platt and Vissers*, 1989; *Rosenbaum*, 2002; *Platt et al*., 2012]. Shortening occurred within the External zones, forming foreland fold and thrust belts, while extension, crustal thinning, and subsidence occurred within the Internal zones and the Alboran Basin [*Platt and Vissers*, 1989; *Vissers et al*., 1995; *Lonergan and White*, 1997; *Torne et al*., 2000; *Faccenna et al*., 2004]. Accretion of the Betic-Rif Internal zones was complete by ~10 Ma [*Rosenbaum*, 2002; *Duggen et al*., 2005]. Since ~7 Ma, however, the Betic-Rif orogen has been progressively uplifted [*Vissers et al*., 1995]. *Duggen et al*. [2005] hypothesized this to be the result of the removal of subcontinental lithosphere and its replacement by more buoyant asthenosphere.

The northeast-southwest trending Atlas mountain belt is the southern edge of the diffuse Africa-Eurasia plate boundary zone. The Middle and High Atlas mountains have been uplifted since ~15–20 Ma [*Ramdani*, 1998; *Missenard et al*., 2006]. The Atlas Mountains now accommodate NNW-SSE Africa-Iberia convergence and are being uplifted at a rate of ~2 mm/yr [*Missenard et al*., 2006; *Stich et al*., 2006].

The widespread Cenozoic volcanic activity in the western Mediterranean provides constraints on the tectonic events described above. The Rif Mountains, Alboran Sea, and Betic Mountains have been affected by igneous activity of variable composition since the Middle Miocene. During the Middle to Upper Miocene subduction related tholeiitic and calc-alkaline volcanism was prevalent throughout the region [*Duggen et al*., 2005]. During the Upper Miocene to Lower Pliocene and Quaternary, igneous activity in southern Iberia and north Africa transitioned to volcanism consisting of alkali basalts, suggesting delamination of continental lithosphere and asthenospheric upwelling beneath southern Iberia and northwestern Africa [*Duggen et al*., 2004, 2005]. The most recent magmatism in the Atlas Mountains includes the eruption of Paleogene to Quaternary alkali basalts within the Middle Atlas.

## 3. Tectonic Models

Numerous tectonic models, summarized by *Calvert et al*. [2000], have been proposed to explain the western Mediterranean tectonic history. These models can be grouped into three broad categories: (1) subduction and slab rollback with or without slab break off [*Royden*, 1993; *Lonergan and White*, 1997], (2) lithospheric convective removal or delamination [*Platt and Vissers*, 1989; *Seber et al*., 1996; *Platt et al*., 2003], and (3) subduction and slab rollback accompanied by lithospheric removal processes [*Duggen et al*., 2004, 2005; *Palomeras et al*., 2014].

The first group of models is supported by multiple tomography studies, which have imaged the mantle structure beneath the Alboran Sea and Gibraltar Arc. These studies revealed high velocities at depths between ~60 and 700 km, which have been interpreted as an oceanic slab present beneath the Alboran Sea and Gibraltar Arc [*Blanco and Spakman*, 1993; *Zeck*, 1996; *Calvert et al*., 2000; *Gutscher et al*., 2002; *Bezada et al*., 2013; *Palomeras et al*., 2014]. The slab rollback accompanied by slab break-off model is supported by the observation that high velocity slab material beneath the Alboran Basin did not appear to extend to the surface [*Blanco and Spakman*, 1993]. Slab detachment was used to explain the uplift of the Betic lithosphere as well as magmatism and anatexis within the Betic Mountains [*Blanco and Spakman*, 1993; *Duggen et al*., 2005]. The most recent *P* wave and Rayleigh wave tomography results from this region, derived from PICASSO and IberArray data, support the slab interpretation [*Bezada et al*., 2013; *Palomeras et al*., 2014]. The evidence for complete slab break-off, however, appears weak as *Bezada et al*. [2013] image a high velocity anomaly beneath the Alboran Sea and southern Spain, extending continuously from ~50 km depth to the transition zone and *Palomeras et al*. [2014] use Rayleigh wave tomography data to show the same high velocity anomaly extending toward the surface.

The second group of models does not involve subduction, but rather removal of gravitationally unstable lithosphere from beneath the Alboran Basin and Gibraltar Arc by either delamination or convective processes [*Seber et al*., 1996; *Calvert et al*., 2000; *Duggen et al*., 2005; *Valera et al*., 2008]. Delamination is as an asymmetric process, analogous to "peeling off" the continental lithosphere causing extension in the overlying crust to migrate in one direction. In contrast, convective removal is supported by the simultaneous,

symmetric extension that occurred throughout the entire Alboran region [*Platt and Vissers*, 1989; *Houseman and Molnar*, 1997; *Platt et al*., 2003].

The third group of models combines subduction and lithospheric removal processes. *Duggen et al*. [2005] and *Palomeras et al*. [2014] used geochemical analysis and surface wave tomography, respectively, to suggest that slab rollback has initiated delamination of the continental mantle lithosphere beneath the Gibraltar Arc. Our research seeks to evaluate these models through a detailed analysis of the lithospheric structure throughout the western Mediterranean.

## 4. Data and Methodology

### 4.1. Receiver Function Method

A Ps (*P* wave to *S* wave, PdS) receiver function (RF) is an approximation of the *S* wave Green's function resulting from *S* conversions from an incident teleseismic *P* wave on the receiver side of the *P* wave path [*Bostock*, 2004; *Rondenay*, 2009]. The individual RF arrivals are *P* to *S* wave (Ps) conversions from seismic impedance discontinuities such as the Moho, the lithosphere-asthenosphere boundary, and the transition zone discontinuities. The positive amplitude arrivals correspond to an increase in seismic impedance with depth (e.g., Moho) and negative amplitudes correspond to a decrease in seismic impedance with depth (e.g., lithosphere-asthenosphere boundary, LAB) [*Langston*, 1979; *Ammon*, 1991]. Deconvolving the vertical component from the horizontal components (radial and tangential), or the longitudinal component from the two orthogonal components, approximately removes the source and receiver response functions from the Ps conversion response. In this study, Ps RFs were calculated using both water-level frequency domain deconvolution [*Burdick and Langston*, 1977] and time-domain iterative deconvolution [*Ligorria and Ammon*, 1999]. We show results from the latter, which uses an iteratively updated spike train as the predicted RF. At each iteration, an estimate of the radial component seismogram is calculated by convolving the predicted RF with the vertical component seismogram. The RF is determined by minimizing the difference between the estimated radial component seismogram and the observed radial seismogram until a predetermined upper error bound is reached.

### 4.2. Data

Ps RFs were calculated from 243 teleseismic earthquakes recorded by 239 broadband seismograph stations from five temporary and permanent seismic networks in southern Iberia and northern Africa, including the PICASSO (Program to Investigate Convective Alboran Sea System Overturn) and IberArray networks (Figure 1b). Station spacing in these arrays ranges from ∼15 to 50 km. Receiver functions were calculated for earthquakes with magnitudes greater than 6.0, which were at source-receiver distances of 30° to 90° (supporting information Figure S1).

### 4.3. Processing

Each receiver function was calculated using three separate Gaussian shaping filters corresponding to 0.5, 1.0, and 2.0 Hz (supporting information Figure S2). At 2 Hz, assuming an average lower crustal Vs of ∼4 km/s and a vertical resolution of $\sim 0.25\lambda$, we are able to resolve lower crustal layering on the ∼0.5 km scale and at 0.5 Hz, layering is resolvable at ∼2 km. Receiver functions that did not achieve an 80% variance reduction were eliminated, as were those that did not have their highest amplitude close to time zero, corresponding to the direct *P* arrival. Additionally, all of the RFs were manually inspected for bad traces. After editing we were left with 6000 high quality receiver functions. These RFs were common conversion point (CCP) stacked [*Dueker and Sheehan*, 1997], to create a 3-D image volume using the depth conversion and spatial repositioning described in *Levander and Miller* [2012]. The image volume bin size chosen for this study was spaced 0.125° × 0.125° laterally and 1 km in depth. Conversion horizons were picked from the image volume along latitude and longitude CCP profiles taken every 0.25°.

The depth conversion and spatial repositioning used the linear tomography assumption: The IASP91 1-D velocity model was used to calculate *P* and *S* wave travel timetables, with 3-D travel time corrections determined from a hybrid 3-D velocity model, which combines the 3-D finite-frequency body wave tomography model of *Bezada et al*. [2013] for mantle structure below 80 km, and the 3-D Rayleigh wave model of *Palomeras et al*. [2014] for structure above 80 km.

*P* wave and *S* wave velocities were obtained from each tomography model by assuming IASP91 Vp/Vs ratios. The average crustal velocities of this 3-D hybrid model range from Vp = 6.43 km/s, Vs = 3.65 km/s in

the western Betic Mountains to Vp = 5.44 km/s, Vs = 3.15 km/s in the Alboran Sea (supporting information Figure S3).

Before the final analysis, we compared the results of the CCP stack with multiple velocity models and Vp/Vs ratios. These models included the 3-D hybrid model discussed above, the IASP91 1-D model with no 3-D correction, and two 3-D models derived from the body wave and surface wave models individually assuming a constant Vp/Vs of 1.73. While the shapes of the major events seen on the resulting CCP profiles remain very consistent between velocity models, the depth to these events is variable. Between the final 3-D hybrid model and the other tested models, there is an average of ~1–3 km difference at ~30–45 km depth and a ~3–6 km difference between ~50 and 80 km depth (supporting information Figure S4).

Hit count maps (supporting information Figure S5) show the number of traces recorded at each grid point in the CCP volume at 45 km and 75 km depth for the 1 Hz RFs. These are the approximate depths of the Moho and deeper lithospheric structure that will be discussed in the following sections. From these maps, we can see good data coverage around the Gibraltar Arc.

### 4.4. Thermobarometry

We also made thermobarometric calculations on 19 volcanic samples distributed throughout Spain and Morocco (Figure 1a). Primitive magma compositions (basalts to basaltic andesites) were compiled from the literature [*El Azzouzi et al*., 1999; *Turner et al*., 1999; *Duggen et al*., 2004, 2005, 2008a, 2008b]. The magmas represent Neogene magmatic centers spanning from the Atlas Mountains in Morocco, northeastward across the Alboran Basin and into southeastern Spain. For thermobarometric analysis [*Lee et al*., 2009], we selected only samples with MgO >8 wt. % and $SiO_2$ > 45 wt. %. Samples with whole-rock atomic Mg/(Mg + $Fe_T$) < 0.55 were then excluded. Because the magma thermobarometers are applicable to magmas derived from peridotites, Zn/$Fe_T$ systematics [*Le Roux et al*., 2010a, 2010b] were examined to exclude those that show extensive clinopyroxene fractionation. Magma compositions were then corrected for olivine fractionation by back addition of equilibrium olivine increments until the magma was in equilibrium with a mantle having an olivine Mg/(Mg + $Fe_T$) of 0.90. We assumed a $Fe^{3+}/Fe_T$ ratio of 0.1. The composition of the primary magma was then inserted into a $SiO_2$-based barometer and MgO-based thermometer to obtain the pressure and temperature of the mantle source of the magma [*Lee et al*., 2009].

## 5. Thermobarometry Results and Interpretations

Magma thermobarometric calculations provide constraints on the temperature and pressures of the magma source region in the mantle throughout the western Mediterranean. We find that calculated temperatures decrease from 1500 to 1270°C toward the north, as do the pressures of equilibrium (Figures 2a and 2b). These estimated temperatures and depths of equilibration most likely represent an average of polybaric melting columns and thus represent maximum bounds on the thickness of the lithosphere. They are consistent with lithospheric thinning beneath the Rif Mountains and an already extremely thinned Alboran Sea. The hottest and deepest magmas occur beneath the Atlas range (Figures 2a–2d). Average mantle potential temperature beneath mid-ocean ridges is between 1300 and 1400°C [*Lee et al*., 2009], hence the 1400–1500°C temperatures beneath the Atlas are anomalously hot. High equilibration pressures suggest deep melting (60–100 km). This is consistent with suggestions that hot plume material may underlie the Atlas Mountains [*Duggen et al*., 2008a]. Beneath the Alboran basin itself, the estimated temperatures and depths of equilibration are ~1350°C and 20 km, not unlike what is seen beneath typical mid-ocean ridges, implying a highly thinned lithosphere beneath the Alboran. Temperatures and depths of equilibration rise again in southeastern Spain. Depths of equilibration are 40–60 km, consistent with thinned continental lithosphere in southeastern Spain. We note that the magmas from this volcanic field are K-rich and have low Nb/La ratios (Figure 2e), suggesting involvement of water in the melting process. Because we have no constraint on the initial water content of these magmas, it is possible that our estimated temperatures and pressures are maximum bounds for the southeastern Spain magma source.

## 6. Receiver Function Observations

The Moho depth map derived from the CCP image volume (Figure 3) shows a highly variable Moho beneath the Gibraltar Arc region with crustal thicknesses ranging from ~25 km in the eastern Betic and Rif

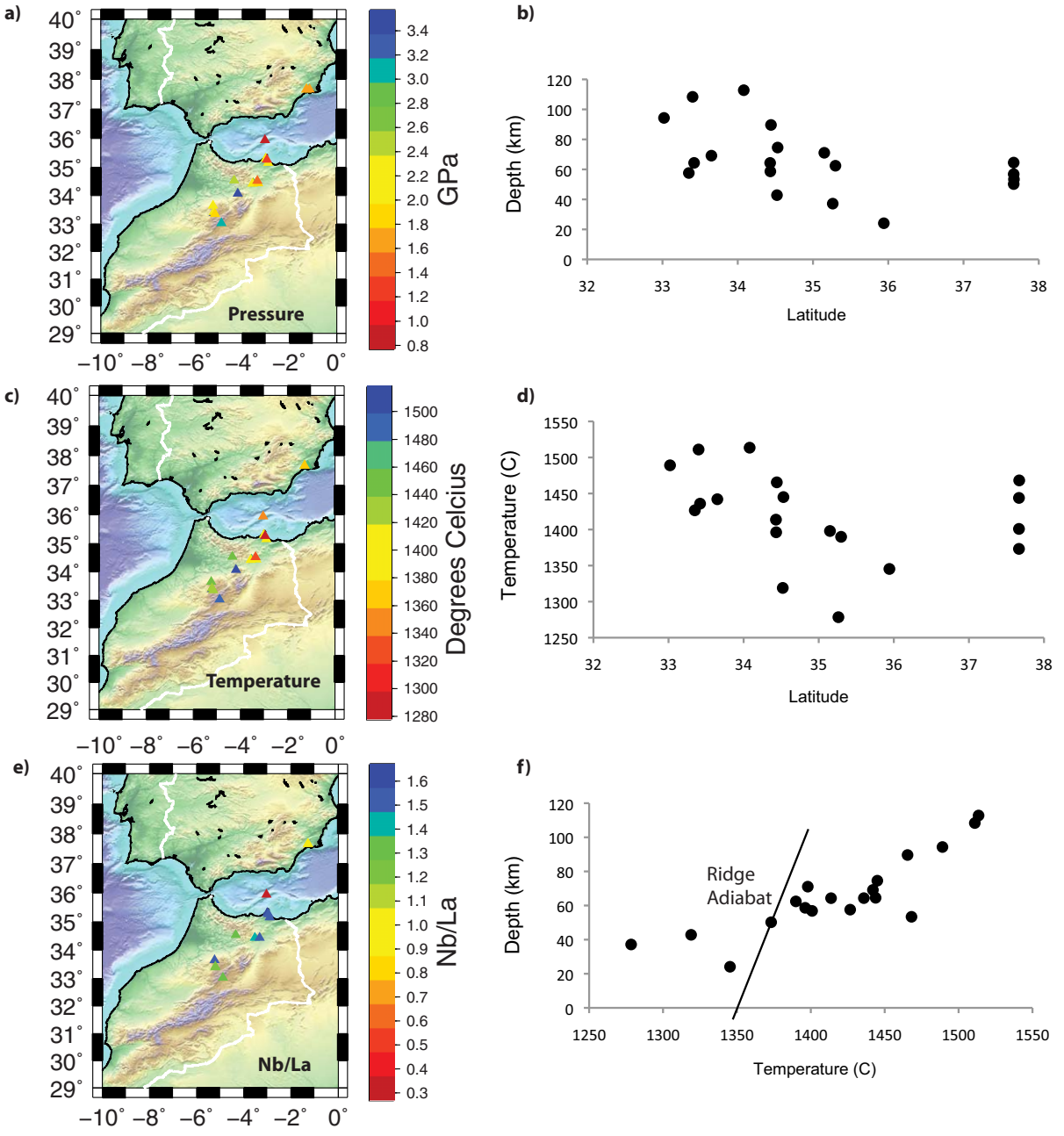


**Figure 2.** (a and b) Map and graph showing decreasing equilibration pressures of estimated primary magmas toward the north. (c and d) Map and graph showing decreasing equilibration temperatures to the north. (e) Map showing low Nb/La ratios in the Alboran Sea and southern Spain. (f) Graph showing temperature and depths (converted from pressure) of equilibration relative to a typical mantle adiabat for mid-ocean ridge mantle. High temperatures toward the south are hotter than typical mid-ocean ridge mantle.

Mountains to over 50 km in the western Betic and Rif Mountains as well as the Gibraltar Strait. The Moho map shows an arcuate shaped crustal root (+45 km) around the Gibraltar Arc. We suggest this crustal root may be the cause of the arcuate shaped negative Bouguer anomaly also seen in the region [*Fullea et al.*, 2010]. The regions of maximum crustal thickness in the central Betics and Rif (~53–55 km) correspond to the largest negative Bouguer anomalies of −120 mGal. *Mancilla et al.* [2012] obtained similar crustal thicknesses with a more limited data set confined to the Betic and Rif Mountains. In the following sections, we provide a detailed description of the crustal and lithospheric structure observed in the CCP volume from each part of the study area.

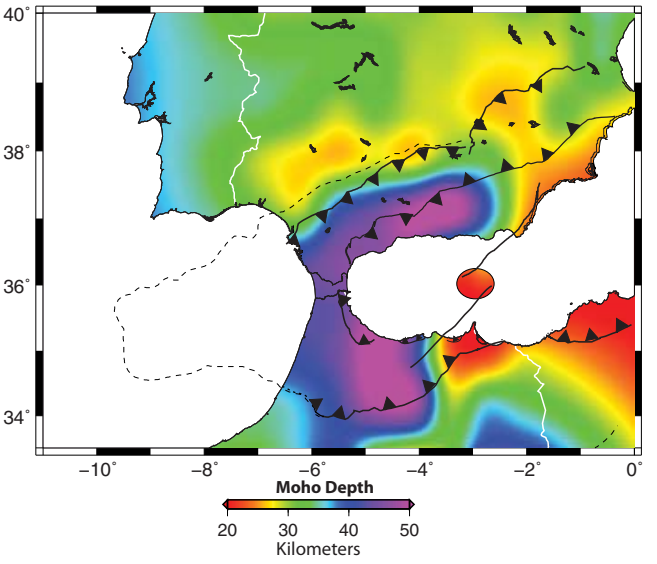


**Figure 3.** Map showing the Moho depth determined from Ps RFs.

### 6.1. Central Spain/Iberian Massif

In central Spain between latitudes 38° and 40°, we identify the Moho as the strong, positive (red) event between ~27 and 35 km depth below sea level (Figures 3 and 4). These depths are consistent with previous active source estimates of ~30–35 km in the Iberian Massif of central Spain [*Simancas et al*., 2003; *Díaz and Gallart*, 2009; *Palomeras et al*., 2009]. We also observe a series of strong negative (blue) events at ~50–100 km depth between −4.5° and −2° longitude, near latitude 38° (Figure 4), which suggest a strong negative velocity gradient under this region. Rayleigh wave tomography along the same profile [*Palomeras et al*., 2014] shows shear velocities decreasing from 4.35 km/s to 4.2 km/s between ~50 and 125 km, consistent with the RF image (Figure 4c). The low velocities are likely associated with the Calatrava Volcanic Province (Figure 1a), an intraplate basaltic volcanic field active from the Late Miocene to the Quaternary, that consists of a series of vents, lava flows, and pyroclastic flows distributed over an area of ~4000 km$^2$ within the Iberian Massif [*Lopez-Ruiz et al*., 1993; *Cebriá and López-Ruiz*, 1995].

Further west and north, the CCP profiles show a series of strong positive and weak negative subMoho events between ~60 and ~100 km depth beneath the Iberian Massif, suggesting strong mantle heterogeneity between −4.5° to −7°W and 39° to 40° N. In an active source seismic study, the *ILIHA DSS Group* [1993] also found upper mantle heterogeneity in the same location, where they observed multiple upper mantle high and low velocity layers between 40 and 90 km depth. *Ayarza et al*. [2010] also find evidence for mantle heterogeneity in this region. They suggest an 11 km thick heterogeneous *P* velocity zone between ~61 and 72 km depth, which they interpret as the spinel-lherzolite to garnet-lherzolite phase transition (Hales interface). It is possible that the positive event seen in Figure 5 at ~65–75 km depth corresponds to this phase transition zone.

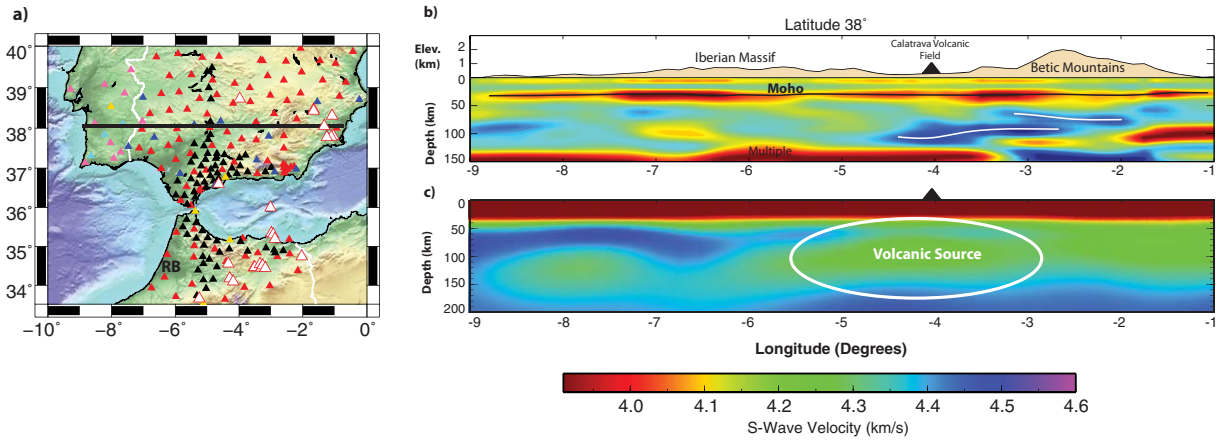


**Figure 4.** (a) Map showing the location of the CCP and surface wave profiles at 38° latitude (black line). (b) 0.5 Hz CCP profile showing consistent crustal thicknesses of ~27–35 km (black line) and strong negative events associated with the Calatrava Volcanic field (white lines). (c) Surface wave profile showing low shear velocities associated with the Calatrava Volcanic field (white circle, surface wave data from *Palomeras et al*. [2014]).

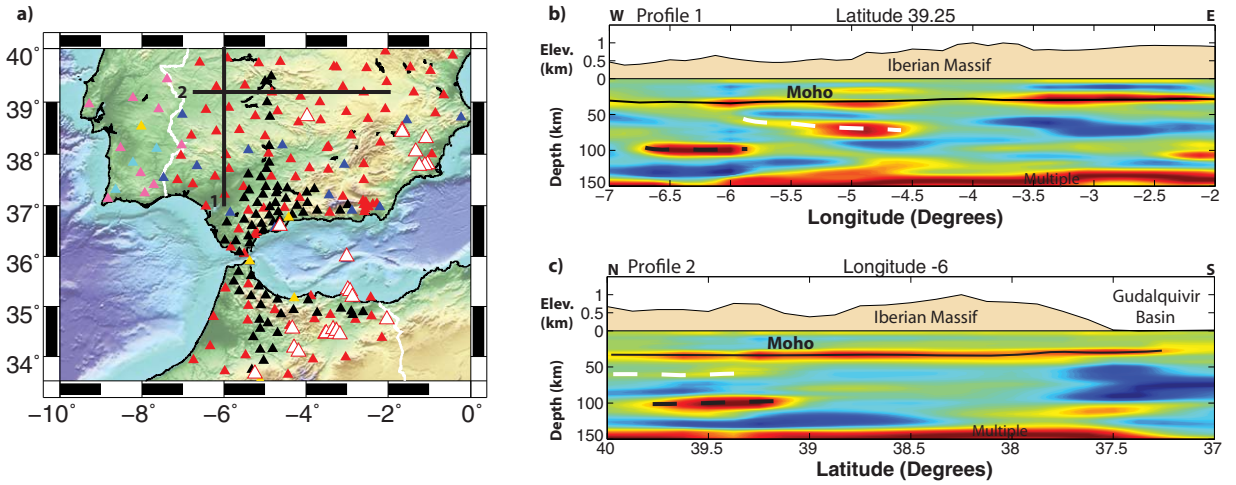


**Figure 5.** (a) Map showing the location of CCP profiles at 39.25° and −6°, marked by the black lines. (b) 1 Hz CCP profile at 39.25°. (c) 1 Hz CCP profiles at −6°. The solid black line marks the Moho depth in both profiles. The white dashed line indicates the shallower positive arrival coinciding with the layer described by *Ayarza et al*. [2010]. The black dashed line indicates the deeper positive arrival, suggesting layering in the mantle down to ∼100 km.

### 6.2. Betic Mountains

The CCP images of the crust beneath the Betic Mountains (Figures 6b–6d) are more complicated than those from the Iberian Massif (Figures 4 and 5). Beneath the Guadalquivir Basin in the west, the RFs show a fairly strong flat Moho signal at ∼30 km, consistent with active source results [*Carbonell et al*., 1998; *Torne et al*., 2000; *Díaz and Gallart*, 2009]. Beneath the western Betics, the Moho signal weakens and dips eastward to ∼45 km depth over a distance of ∼50 km. Under the central and eastern Betics, the Moho signal strengthens and dips slightly eastward to ∼53 km. Below the Moho in the central Betics, a second positive event

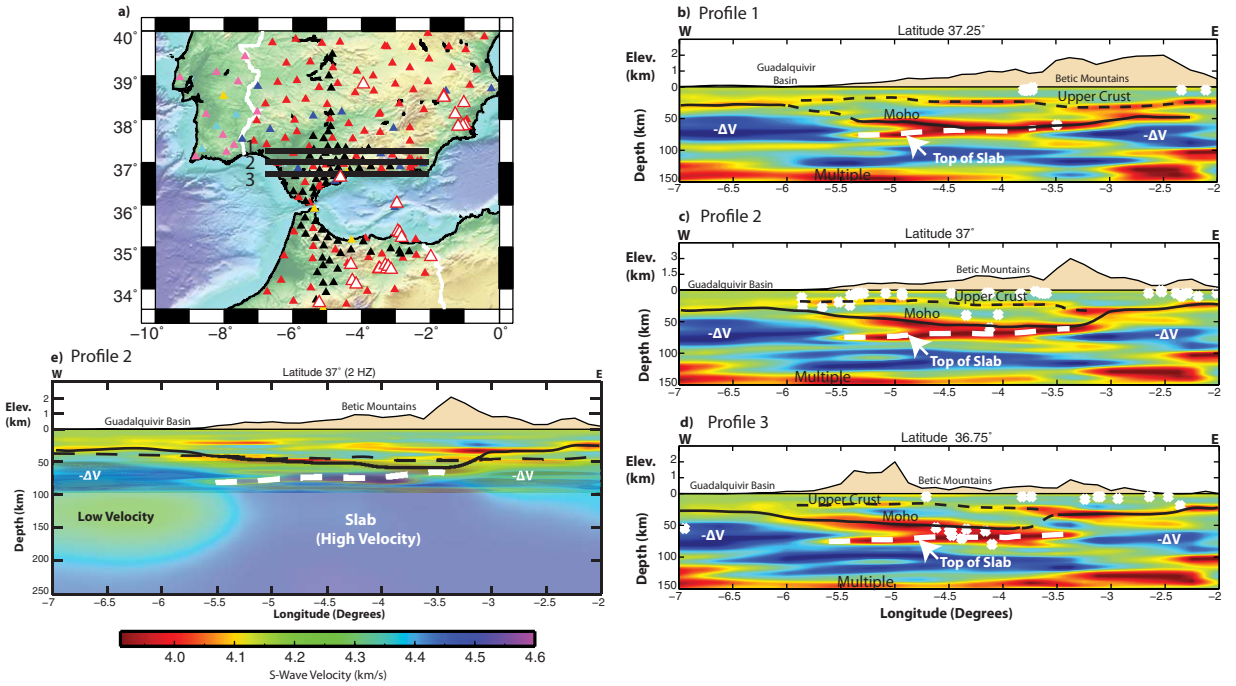


**Figure 6.** (a) Map showing the location of CCP profiles at 37.25°, 37°, and 36.75° latitude, marked by the black lines. (b) 1 Hz CCP profile at latitude 37.25°. (c) 1 Hz CCP profile at latitude 37°. (d) 1 Hz CCP profile at latitude 36.75°. The black dashed line marks a strong midcrustal event. The black solid line marks the continental Moho. The deepest, positive event, interpreted as the top of the slab, is marked by the white dashed line. The white diamonds mark earthquake hypocenter locations. −ΔV indicates the locations where strong negative events suggest a negative velocity gradient. (e) The 2 Hz receiver functions and the Rayleigh wave tomography results along latitude 37°. We can see that the deep positive RF event coincides with the top of the high velocity slab and the strong negative events in the west and east coincide with the tops of low velocity zones seen in the surface waves.

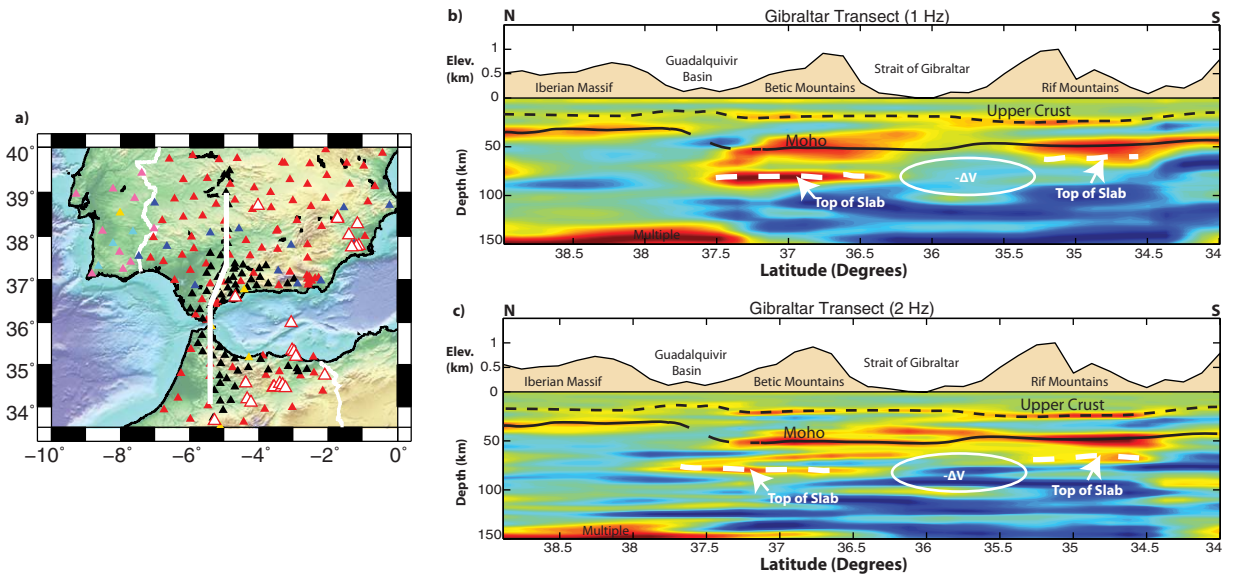


**Figure 7.** (a) Map showing the location of the north-south CCP profile extending from the Iberian Massif, through the Betic Mountains, across the Gibraltar Strait, and into the Rif Mountains (white line). (b) 1 Hz CCP profile. (c) 2 Hz CCP profile. The black dashed line indicates the shallow midcrustal arrival. The Moho is marked by the solid black line. The white dashed line indicates the signal from the top of the slab. The white circle outlines the region where we see a negative RF event rather than a strong positive arrival between ~70 and 80 km depth.

extends from ~80 km depth in the west up to ~53 km depth in the east, where it intersects the shallower Moho event. Based on surface wave tomography, we correlate the deeper positive event with the top of the Alboran slab (Figure 6e). This pair of intersecting RF horizons (Moho and top of slab) is visible under the central Betics between 36.75° and 37.25° latitude (Figures 6b–6d). The CCP profiles show, however, that the events appear closer together and the "top of slab" event extends laterally over a smaller distance toward the north.

In the eastern Betic Mountains, where the two events intersect, the combined positive event becomes weak and discontinuous as it shallows from ~53–55 km to ~25–35 km. On both the east and west sides of the deep RF event pair, we observe strong negative horizons at ~50 and ~80 km depth, directly below the shallowing Moho signal beneath the western and eastern Betics (Figures 6b–6e).

### 6.3. Gibraltar Strait/Alboran Sea

In 1 Hz and 2 Hz CCP profiles across the Strait of Gibraltar (Figure 7), we identify a variable strength midcrustal event at 25–30 km depth, extending from the Iberian Massif across the Gibraltar Strait into the Rif Mountains. The Moho is discontinuous: We identify the strong, flat Moho signal beneath the Iberian Massif at 30–35 km (Figure 5), and the strong Moho event under the western Betics at ~50 km (Figure 6) which we can trace in the 2 Hz CCP profile under the strait of Gibraltar and into the Rif. The Moho is not imaged under the Guadalquivir Basin. The positive event at ~80 km depth under the Betics, which we associate with the Alboran slab, is clearly visible as is a similar event at ~70 km beneath the Rif. We note the absence of a strong positive event at ~70–80 km depth beneath the Strait of Gibraltar.

The crustal thickness beneath the central Alboran Sea was determined using data from the seismic station ES.EALB on Alboran island (35.9°N, −3.0°W; Figure 1b). Receiver functions in each frequency band indicate a very shallow Moho, ~15 km depth, in this region (Figure 3). Thermobarometric analysis of magmas from this region indicates that beneath the Alboran basin the estimated temperatures and depths of equilibration are ~1350°C and 20 km (Figures 2a–2d), implying a highly thinned lithosphere in this region.

### 6.4. Rif Mountains

The complicated crustal structure of the southern Betics and the Strait of Gibraltar extends into northern Rif Mountains of Morocco where a shallow midcrustal event is seen near ~25 km depth beneath much of the western and central Rif Mountains. We identify the Moho as the strong positive event at ~45–50 km depth beneath the Rharb Basin and western Rif Mountains. As under the Betics, the Moho beneath the central Rif dips and intersects a deeper positive event with a maximum depth of about ~70 km. Again, we use surface

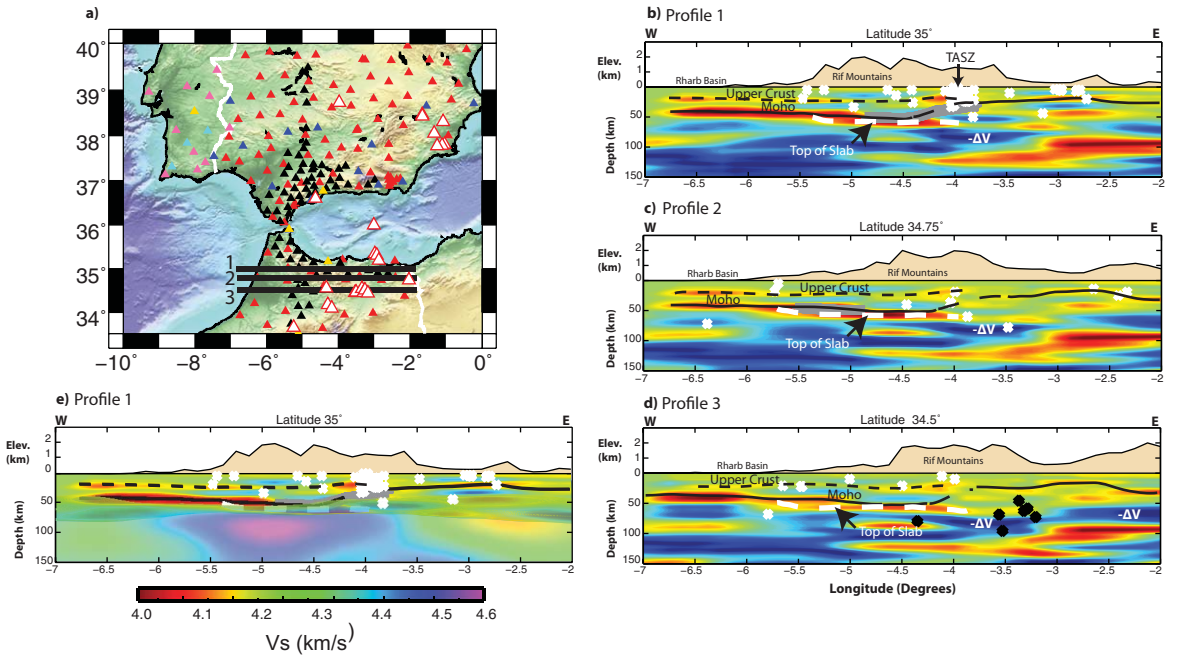


**Figure 8.** (a) Map showing the location of CCP profiles at 35°, 34.75°, and 34.5° latitude, marked by the black lines. White triangles indicate locations of Cenozoic volcanic fields from which samples were used for geochemical analysis. (b) 1 Hz CCP profiles at latitude 35°. (c) 1 Hz CCP profiles at latitude 34.75°. (d) 1 Hz CCP profiles at latitude 34.5°. (e) The receiver functions and the Rayleigh wave tomography results along latitude 35°. We can see that the deep positive RF event coincides with the top of the high velocity slab and the strong negative events in the west and east coincide with the tops of low velocity zones seen in the surface waves. The black short-dashed line marks a strong midcrustal event. The black solid line marks the Moho. The black long-dashed line marks the weak discontinuous Moho seen in the eastern Rif. The deeper, positive event, interpreted as the top of the slab, is marked by the white dashed line. The white diamonds mark earthquake hypocenter locations. The black diamonds mark the melting depths of basalts sampled from the region. The gray bold line marks the Moho depth taken from active source results.

wave tomography to correlate the deeper positive event with the top of the Alboran slab (Figure 8e). This pair of RF events is visible as far south as 34.25° between −5.5° and −3.75° longitude (Figures 8b–8d). In the eastern Rif, the deep event disappears while the Moho weakens, in places is discontinuous, and shallows from ∼50 km to ∼25–30 km. The Moho depths beneath the western and eastern Rif agree well with preliminary estimates of crustal thickness from the PICASSO-related refraction profiles RIFSIS [*Gil et al.*, 2013]. Figure 8 shows close correlation between the Moho depth determined from refraction plotted (bold gray line) and the Moho on the CCP profiles (black lines).

Last, we see a strong negative event at 60–80 km depth beneath the thinned crust of the eastern Rif between 4.25°W and 3°W, which lies beneath the Guilliz volcanic field. Thermobarometric analysis of basalts from this field indicate mantle melting depths between 40 and 60 km, suggesting a very thin lithosphere in the region.

## 7. Discussion

### 7.1. Comparison With Surface Wave Tomography

Here we discuss the RF results in comparison to a recent Rayleigh wave tomography velocity model [*Palomeras et al.*, 2014]. As we noted above, the deepest positive RF events beneath the Betics and Rif are correlated with the top of the high velocity Alboran slab imaged by both surface wave tomography and body wave tomography. These studies indicate that at depth this slab has an arcuate shape, and extends from the northern Rif Mountains in Morocco to the Betic Mountains in southern Spain, extending into the transition zone [*Bezada et al.*, 2013]. Figures 6e and 8e compare CCP profiles across the Betic and Rif Mountains with the corresponding Rayleigh wave tomography profiles [*Palomeras et al.*, 2014]. In addition to the positive signal from the top of the slab, the strong negative signals in the western and eastern Betics coincide with the tops of low velocity zones seen on both sides of the Alboran slab. Figure 9a shows a slice at 75 km depth from the surface wave results, where we see a strong, high velocity slab anomaly beneath the entire Gibraltar Arc and western Alboran Sea. On top of this velocity depth slice, we show Moho depth contours of

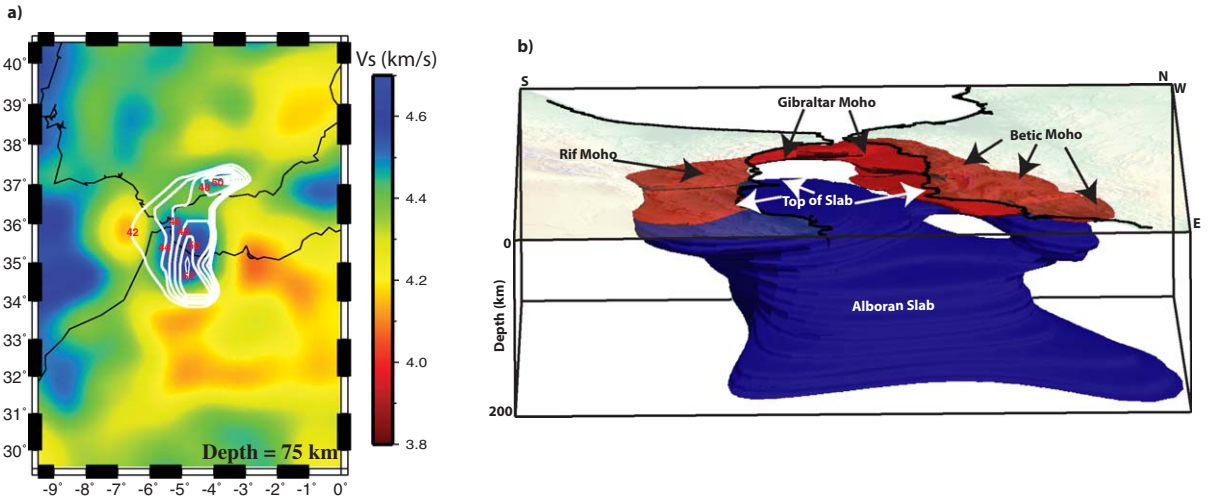


**Figure 9.** (a) Depth slice at 75 km from the Rayleigh wave tomography model, showing the high velocity body beneath the Gibraltar Arc. White lines show contours of Moho depth for the region of thickened crust as seen in Figure 3. (b) 3-D image of the deep receiver function signal (red) and the high velocity slab material imaged by the surface wave tomography (blue). It is clear that the deepest extent of the receiver function feature coincides with the shallowest extent of the high velocity slab.

the thickened crust as seen in the Moho map (Figure 3), demonstrating that the thickened crust and the slab anomaly coincide.

Figure 9b is a 3-D image showing the Moho and subcrustal (∼70–80 km depth) positive RF arrival beneath the Gibraltar Arc as a red isosurface at the 50% level, and the Alboran slab as a blue isosurface (at 4.5 km/s). The subcrustal RF signal coincides with the high velocities that define the top of the Alboran slab. These images provide compelling evidence that the deep positive RF events observed beneath the Betics, the Gibraltar Strait, and the central Rif are all conversions from the top of the Alboran slab.

### 7.2. Delamination of Continental Lithosphere

As described in the previous sections, we observe a single RF event at ∼30–45 km depth beneath the western Rif Mountains (Figure 8). We interpret this RF event as the continental Moho. In both the central Rif and Betic Mountains, we observe two intersecting positive events, the shallower of which corresponds to the Moho, and the deeper of which corresponds to the top of the Alboran slab. We interpret these intersecting RF events as evidence of ongoing lithospheric detachment. The unusually thick crust (∼45–55 km, Figure 3, 6, and 8) results from a depression of the continental lithosphere caused by the load of the descending slab, which *Valera et al.* [2008] suggest may be enough to initiate delamination of the lower continental crust and mantle lithosphere.

Hypocenter locations for earthquakes ($M > 4.5$) occurring within the Betic and Rif Mountains are shown in Figures 6 and 8. In the Betic Mountains, seismicity appears concentrated along 36.75°N between the two positive RF events (Figure 6d), which we interpret as deformation associated with lithospheric detachment. In the Rif Mountains, along 35°N (Figure 8b), a concentration of earthquake activity coincides with the location where the Trans Alboran Shear Zone (TASZ) intersects the northern coast of Morocco near 4°W, where the deeper RF event disappears. Focal mechanisms indicate that much of this seismic activity can be attributed to nearly vertical motion initiated by a slab pull [*Buforn et al.*, 1995; *Seber et al.*, 1996; *Morales et al.*, 1997; *Wortel and Spakman*, 2000].

In the eastern Rif and the eastern and western Betic Mountains, the deep RF event pairs transition to a single weak RF event as the crust thins from ∼50 to ∼ 30 km depth. Thermobarometric analysis of basalts from the eastern Rif indicate shallow melting depths between ∼40 and ∼80 km (Figure 8d), directly below the thinning crust, coincident with the strong negative events observed at ∼50–60 km depth beneath the eastern Rif and at either end of the Betics. We suggest that the volcanism is evidence of recently removed lithosphere, and that the strong negative events represent asthenosphere that has replaced the delaminated slab. The deep, top of the slab event, therefore, represents the impedance contrast between the high velocity slab lithosphere and the low velocity asthenosphere that has filled the delaminated region.

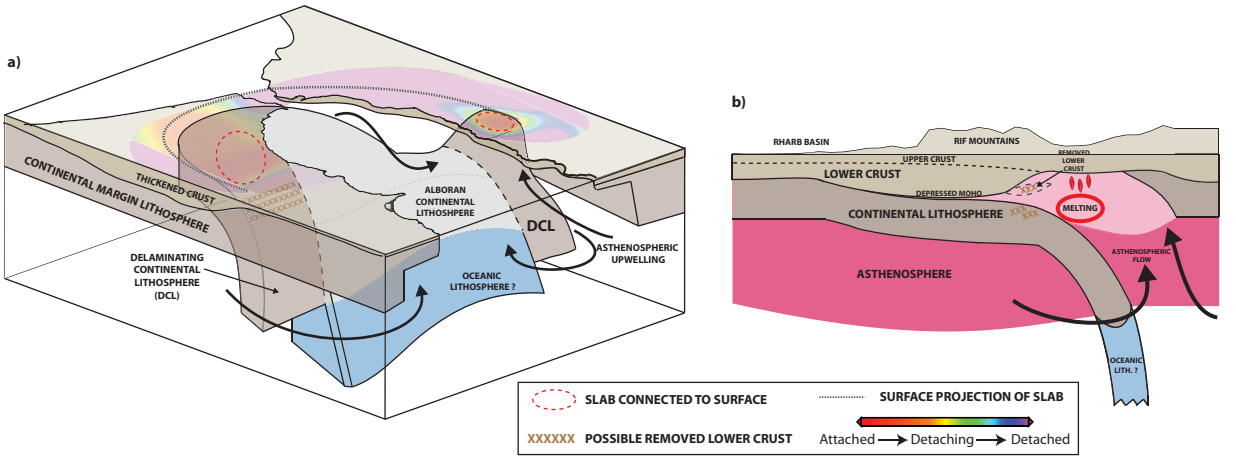


**Figure 10.** (a) 3-D cartoon showing the geometry of the slab beneath the Gibraltar Arc. The dotted line along the surface shows the surface projection of the slab. The color contours indicate where the slab remains attached to the continental lithosphere and where it has detached. (b) Cartoon of a profile across the Rif Mountains showing east to west delamination of the continental lithosphere.

We have interpreted the weak, shallow RF event directly above the low velocity zones as the continental Moho. The sharp decrease in crustal thickness suggests possible removal of a portion of the lower crust along with the continental lithospheric mantle. The weak character of this signal may be caused by the dip of the interface since the common-conversion point stacking method assumes that PdS conversions are generated by horizontal discontinuities and does not account for scattering of the PdS conversion that may occur at dipping interfaces. However, this shallow signal is weak even where flat in the easternmost Rif and on both sides of the Betics. This may be caused by a decrease in impedance contrast at the Moho, resulting from the emplacement of asthenosphere at or near the base of the crust where continental lithosphere has been removed with accompanying basaltic dike emplacement in the lowermost crust. The surface wave tomography results indicate a small velocity contrast from the crust (depth slice 25 km), where Vs is ~3.8 km/s to the upper mantle (depth slices 35 and 50 km) where Vs is ~4.1–4.2 km/s [*Palomeras et al*., 2014]. A joint inversion of the RF and surface wave data sets will better constrain the velocity contrast associated with the shallow Moho boundary, but is beyond the scope of this paper.

We suggest that delamination of the continental margin lithosphere was initiated when oceanic lithosphere was consumed by subduction and slab rollback. The load on the continental margin resulting from the Alboran slab is depressing the Moho beneath the Rif and Betic Mountains, initiating lithospheric detachment, and permitting asthenosphere to replace lithosphere at shallow depths (Figure 10). The presence of asthenospheric material at subcrustal depths may be responsible for the recent uplift of the Betic Mountains.

This model is similar to that proposed by *Duggen et al*. [2005] for the western Mediterranean. Additionally, *Garcia-Castellanos and Villasenor* [2011] use a lithospheric delamination and slab tear model to explain the Messinian salinity crisis and the cyclicity observed in early salt deposits in the western Mediterranean. In North America, *Levander et al*. [2011] noted that a similar set of observations show crustal detachment at the top of a lithospheric drip beneath the Colorado Plateau.

### 7.3. Attached Versus Detached Slab

The deep RF events seen in the central Betics appear to merge with the Moho between −4.5°W and −3.5°W along the northernmost profile at 37.25°N (Figure 6b). In the central profile (Figure 6c), the two positive events merged over an even shorter distance near −3.5°W, and in the southernmost profile at 36.75°N the two events appear nearly completely separated (Figure 6d). We suggest that the slab is still attached to the crust beneath a portion of the central Betic Mountains, likely where the Moho reaches its maximum depth of ~53 km, and that the seismicity at and below the Moho reflects the ongoing detachment.

In the Gibraltar Strait, we do not observe a deep top of the slab RF event in the CCP profile. Instead we see negative events below the Moho (Figure 7), in agreement with both the *P* wave and Rayleigh wave tomography images that indicate the subducting slab is not as shallow beneath the Gibraltar Strait as along the

adjacent continental margins [*Bezada et al*., 2013; *Palomeras et al*., 2014]. The surface wave tomography shows low *S* wave velocities (~4.1 km/s) down to ~60 km depth [*Palomeras et al*., 2014], suggesting that the subducting slab has already detached from the crust and has been replaced by asthenosphere.

In contrast to the Betics, the deep RF events in the central Rif Mountains are very close together everywhere but near their eastern end (~4°W), suggesting that the slab remains attached beneath a large portion of the central Rif. This is in agreement with geodetic modeling of GPS data [*Perouse et al*., 2010] that suggests that the Alboran slab is still attached to the Rif crust. We suggest that the maximum Moho depths (~53 km) beneath the central Betic and Rif Mountains correspond to places where the slab remains attached to the base of the continental lithosphere.

## 8. Conclusions

Ps receiver functions and thermobarometric constraints from late Cenozoic basalts in the western Mediterranean provide evidence for ongoing lithospheric delamination beneath the Gibraltar Arc, with the detachment surface being the continental Moho. Beneath the central Betic and Rif Mountains, we see both a strong Moho and an intersecting dipping strong, positive mantle event which we interpret as the top of the Alboran Sea slab imaged previously by surface wave tomography [*Palomeras et al*., 2014]. We interpret the intersection of the Moho and upper mantle event from the top of the Alboran slab to be indicative of ongoing lithospheric delamination. The RF images reveal a highly variable Moho with depths ranging from ~53 km in the western Betic and Rif Mountains where the slab is still attached, to ~20–25 km in the eastern Betic and Rif Mountains and the central Alboran Sea where the slab appears to have already detached. Detachment is being driven by the slab-pull force due to the load of the sinking Alboran Sea slab.

In addition to thinner crust, in the eastern Rif and the eastern and western Betics, we observe negative polarity mantle RF events, which we interpret as a shallow, recently formed, post-detachment LAB. Thermobarometric analysis of basalts indicate shallow mantle melting depths of 40–60 km in the eastern Rif, the eastern Betics, and the central Alboran Sea, supporting the interpretation of recent lithospheric thinning and removal. The surface volcanics and shallow LAB are indicative of decompression melting that has accompanied the upwelling asthenosphere that replaces the Alboran slab.

We conclude that at the end of oceanic subduction rollback, the edges of the Alboran slab began detaching from adjacent continental margins. The Alboran slab has detached from the base of the crust beneath the eastern Betic and Rif Mountains, is still attached the central Betic and Rif Mountains, and has already detached from the western Betic Mountains, and the Strait of Gibraltar.

**Acknowledgments**

This research was funded by the U.S. National Science Foundation EAR-0808939. The deployment of the IberArray broadband seismic network is part of the CONSOLIDER CSD2006-00041 (Geosciences in Iberia: Integrated studies on Topography and 4D Evolution) grant from the Spanish Ministry of Science and Innovation. Additional funding was provided by the Spanish ministry under grants CGL2010–17280 and by Generalitat de Catalunya under grant 2009 SGR 6. We thank the IRIS data management center, the Instituto Geografico Nacional (Spain), the Instituto de Meteorologia (Portugal), the Centro de Geofisica da Universidade de Lisboa (Portugal), and the Universidad Complutense de Madrid (Spain) for contributing data to this study. We thank the Seismology and Tectonics At Rice (STAR) group for valuable discussions.

## References

Ammon, C. (1991), The isolation of receiver effects from teleseismic P waveforms, *Bull. Seismol. Soc. Am.*, *81*(6), 2504–2510.

Ayarza, P., I. Palomeras, R. Carbonell, J. C. Afonso, and F. Simancas (2010), A wide-angle upper mantle reflector in SW Iberia: Some constraints on its nature, *Phys. Earth Planet. Inter.*, *181*(3–4), 88–102, doi:10.1016/j.pepi.2010.05.004.

Bezada, M. J., E. D. Humphreys, D. R. Toomey, M. Harnafi, J. M. Dávila, and J. Gallart (2013), Evidence for slab rollback in westernmost Mediterranean from improved upper mantle imaging, *Earth Planet. Sci. Lett.*, *368*, 51–60, doi:10.1016/j.epsl.2013.02.024.

Blanco, M. J., and W. Spakman (1993), The P-wave velocity structure of the mantle below the Iberian Peninsula: Evidence for subducted lithosphere below southern Spain, *Tectonophysics*, *221*, 13–34.

Bostock, M. G. (2004), Green's functions, source signatures, and the normalization of teleseismic wave fields, *J. Geophys. Res.*, *109*, B03303, doi:10.1029/2003JB002783.

Buforn, E., C. S. De Galdeano, and A. Udlas (1995), Seismotectonics of the Ibero-Maghrebian region, *Tectonophysics*, *248*, 247–261.

Burdick, L. J., and C. A. Langston (1977), Modeling crustal structure through the use of converted phases in teleseismic body-wave forms, *Bull. Seismol. Soc. Am.*, *67*(3), 677–691.

Calvert, A., E. Sandvol, D. Seber, M. Barazangi, S. Roecker, T. Mourabit, F. Vidal, G. Alguacil, and N. Jabour (2000), Geodynamic evolution of the lithosphere and upper mantle beneath the Alboran region of the western Mediterranean: Constraints from travel time tomography, *J. Geophys. Res.*, *105*, 10,871–10,898.

Carbonell, R., V. Sallarés, and J. Pous (1998), A multidisciplinary geophysical study in the Betic chain (southern Iberia Peninsula), *Tectonophysics*, *288*, 137–152.

Cebriá, J.-M., and J. López-Ruiz (1995), Alkali basalts and leucitites in an extensional intracontinental plate setting: The late Cenozoic Calatrava Volcanic Province (central Spain), *Lithos*, *35*(1–2), 27–46, doi:10.1016/0024-4937(94)00027-Y.

Díaz, J., and J. Gallart (2009), Crustal structure beneath the Iberian Peninsula and surrounding waters: A new compilation of deep seismic sounding results, *Phys. Earth Planet. Inter.*, *173*(1–2), 181–190, doi:10.1016/j.pepi.2008.11.008.

Dueker, K., and A. Sheehan (1997), Mantle discontinuity structure from midpoint stacks of converted P to S waves across the Yellowstone hotspot track, *J. Geophys. Res.*, *103*, 7153–7169.

Duggen, S., K. Hoernle, P. van den Bogaard, and C. Harris (2004), Magmatic evolution of the Alboran region: The role of subduction in forming the western Mediterranean and causing the Messinian Salinity Crisis, *Earth Planet. Sci. Lett.*, *218*(1–2), 91–108, doi:10.1016/S0012-821X(03)00632-0.

Duggen, S., K. Hoernle, P. Van Den Bogaard, and D. Garbe-Schonberg (2005), Post-collisional transition from subduction- to intraplate-type magmatism in the Westernmost Mediterranean: Evidence for continental-edge delamination of subcontinental lithosphere, *J. Petrol.*, *46*(6), 1155–1201, doi:10.1093/petrology/egi013.

Duggen, S., K. Hoernle, P. Van den Bogaard, and D. Garbe-Schonberg (2008a), Flow of Canary mantle plume material through a subcontinental lithospheric corridor beneath Africa to the Mediterranean, *Geology*, *37*, 283–286.

Duggen, S., K. Hoernle, A. Klugel, J. Geldmacher, M. Thirwall, F. Hauff, D. Lowry, and N. Oates (2008b), Geochemical zonation of the Miocene Alboran Basin volcanism (westernmost Mediterranean): Geodynamic implications, *Contrib. Mineral. Petrol.*, *156*, 1155–1201.

El Azzouzi, M., J. Bernard-Griffiths, H. Bellon, R. C. Maury, A. Pique, S. C. Fourcade, and J. Hernandez (1999), Evolution of the sources of Moroccan volcanism during the Neogene, *C. R. Acad. Sci.*, *329*, 95–102.

Faccenna, C., C. Piromallo, A. Crespo-Blanc, L. Jolivet, and F. Rossetti (2004), Lateral slab deformation and the origin of the western Mediterranean arcs, *Tectonics*, *23*, TC1012, doi:10.1029/2002TC001488.

Fullea, J., M. Fernandez, J.C. Afonso, J. Verges, and H. Zeyen (2010), The structure and evolution of the lithosphere-asthenosphere boundary beneath the Atlantic-Mediterranean Transition Region, *Lithos*, *120*, 74–95, doi:10.1016/j.lithos.2010.03.003.

Garcia-Castellanos, D., and A. Villaseñor (2011), Messinian salinity crisis regulated by competing tectonics and erosion at the Gibraltar arc, *Nature*, *480*(7377), 359–363, doi:10.1038/nature10651.

Gil, A., J. Gallart, J. Diaz, R. Carbonell, M. Harnafi, and A. Levander (2013), Crust structure across the Rif Cordillera from 'RIFSIS' seismic refraction and wide-angle reflection experiment, paper presented at EGU General Assembly, Eur. Geosci. Union, Vienna, Austria.

Gutscher, M., J. Malod, J. Rehault, F. Klingelhoefer, L. Mendes-Victor, and W. Spakman (2002), Evidence for active subduction beneath Gibraltar, *Geology*, *30*(12), 1071–1074, doi:10.1130/0091-7613(2002)030<1071.

Houseman, G., and P. Molnar (1997), Gravitational (Rayleigh-Taylor) instability of a layer with non-linear viscosity and convective thinning of continental lithosphere, *Geophys. J. Int.*, *128*(1), 125–150, doi:10.1111/j.1365-246X.1997.tb04075.x.

ILIHA DSS Group (1993), A deep seismic sounding investigation of lithospheric heterogeneity and anisotropy beneath the Iberian Peninsula, *Tectonophysics*, *221*, 35–31.

Langston, C. A. (1979), Structure under Mount Rainier, Washington, inferred from teleseismic body waves, *J. Geophys. Res.*, *84*, 4749–4762.

Lee, C.-T.A., P. Luffi, T. Plank, H. A. Dalton, and W. P. Leeman (2009), Constraints on the depths and temperatures of basaltic magma generation on Earth and other terrestrial planets using new thermobarometers for mafic magmas, *Earth Planet. Sci. Lett.*, *279*, 20–33.

Le Roux, V., R. Dasgupta, and C.-T. A. Lee (2010a), First series transition metals (Zn, Fe, Mn, Co, Sc, V) as tracers of mineralogical heterogeneities in the mantle, *Geochimica et Cosmochimica Acta*, *74*, A582.

Le Roux, V., C.-T.A. Lee, and S. J. Turner (2010b), Zn/Fe systematics in mafic and ultramafic systems: Implications for detecting major element heterogeneities in the Earth's mantle, *Geochim. Cosmochim. Acta*, *74*, 2779–2796.

Levander, A., B. Schmandt, M. S. Miller, K. Liu, K. E. Karlstrom, R. S. Crow, C.-T. A. Lee, and E. D. Humphreys (2011), Continuing Colorado plateau uplift by delamination-style convective lithospheric downwelling, *Nature*, *472*(7344), 461–465, doi:10.1038/nature10001.

Levander, A., and M. Miller (2012), Evolutionary aspects of lithosphere discontinuity structure in the western U.S., *Geochem. Geophys. Geosyst.*, *13*, Q0AK07, doi:10.1029/2012GC004056.

Ligorria, P., and C. J. Ammon (1999), Iterative deconvolution and receiver-function estimation, *Bull. Sesimol. Soc. Am.*, *89*(5), 1395–1400.

Lonergan, L., and N. White (1997), Origin of the Betic-Rif mountain belt, *Tectonics*, *16*, 504–522, doi:10.1029/96TC03937/full.

Lopez-Ruiz, J., J. M. Cebria, M. Doblas, R. Oyarzun, M. Hoyos, and C. Martin (1993), Cenozoic intra-plate volcanism related to extensional tectonics at Calatrava, central Iberia, *J. Geol. Soc. London*, *150*(5), 915–922, doi:10.1144/gsjgs.150.5.0915.

Mancilla, F., et al. (2012), Crustal thickness variations in northern Morocco, *J. Geophys. Res.*, *117*, B02312, doi:10.1029/2011JB008608.

Missenard, Y., H. Zeyen, D. Frizon de Lamotte, P. Leturmy, C. Petit, M. Sébrier, and O. Saddiqi (2006), Crustal versus asthenospheric origin of relief of the Atlas Mountains of Morocco, *J. Geophys. Res.*, *111*, B03401, doi:10.1029/2005JB003708.

Morales, J., I. Serrano, F. Vidal, and F. Torcal (1997), The depth of the earthquake activity in the Central Betics (Southern Spain), *Geophys. Res. Lett.*, *24*, 3289–3292.

Palomeras, I., et al. (2009), Nature of the lithosphere across the Variscan orogen of SW Iberia: Dense wide-angle seismic reflection data, *J. Geophys. Res.*, *114*, B02302, doi:10.1029/2007JB005050.

Palomeras, I., S. Thurner, A. Levander, K. Liu, A. Villasenor, R. Carbonell, and M. Harnafi (2014), Finite-frequency Rayleigh wave tomography of the western Mediterranean: Mapping its lithospheric structure, *Geochem. Geophys. Geosyst.*, *15*, 140–160, doi:10.1002/2013GC004861.

Perouse, E., P. Vernant, J. Chery, R. Reilinger, and S. McClusky (2010), Active surface deformation and sub-lithospheric processes in the western Mediterranean constrained by numerical models, *Geology*, *38*, 823–826, doi:10.1130/G30963.1.

Platt, J., and R. Vissers (1989), Extensional collapse of thickened continental lithosphere: A working hypothesis for the Alboran Sea and Gibraltar arc, *Geology*, *17*, 540–543, doi:10.1130/0091-7613(1989)017<0540.

Platt, J., M. Whitehouse, and S. Kelley (2003), Simultaneous extensional exhumation across the Alboran Basin: Implications for the causes of late orogenic extension, *Geology*, *31*, 251–254, doi:10.1130/0091-7613(2003)031<0251.

Platt, J. P., W. M. Behr, K. Johanesen, and J. R. Williams (2012), The Betic-Rif arc and its Orogenic Hinterland: A review, *Annu. Rev. Earth Planet. Sci.*, *41*(1), 313–357, doi:10.1146/annurev-earth-050212-123951.

Ramdani, F. (1998), Geodynamic implications of intermediate-depth earthquakes and volcanism in the intraplate Atlas mountains (Morocco), *Phys. Earth Planet. Inter.*, *108*, 245–260.

Rondenay, S. (2009), Upper mantle imaging with array recordings of converted and scattered teleseismic waves, *Surv. Geophys.*, *30*(4–5), 377–405, doi:10.1007/s10712-009-9071-5.

Rosenbaum, G. (2002), Reconstruction of the tectonic evolution of the western Mediterranean since the Oligocene, *J. Virtual Explor.*, *8*, 107–130.

Royden, L. H. (1993), Evolution of retreating subduction boundaries formed during continental collision, *Tectonics*, *12*, 629–638, doi: 10.1029/92TC02641.

Seber, D., M. Barazangi, A. Ibenbrahimt, and B. Ahmed (1996), Geophysical evidence for lithospheric delamination beneath the Alboran Sea and Hif-Betic mountains, *Nature*, *379*, 785–790.

Simancas, J. F., et al. (2003), Crustal structure of the transpressional Variscan orogen of SW Iberia: SW Iberia deep seismic reflection profile (IBERSEIS), *Tectonics*, *22*, 1062, doi:10.1029/2002TC001479.

Stich, D., E. Serpelloni, F. de Lis Mancilla, and J. Morales (2006), Kinematics of the Iberia–Maghreb plate contact from seismic moment tensors and GPS observations, *Tectonophysics*, *426*(3–4), 295–317, doi:10.1016/j.tecto.2006.08.004.

Torne, M., M. Fernandez, M. Comas, and J. Soto (2000), Lithospheric structure beneath the Alboran Basin: Results from 3D gravity modeling and tectonic relevance, *J. Geophys. Res.*, *105*, 3209–3228.

Turner, S., J. P. Platt, R. M. M. George, S. P. Kelley, D. G. Pearson, and G. M. Nowell (1999), Magmatism associated with orogenic collapse of the Betic-Alboran Domain, SE Spain, *J. Petrol.*, *40*, 1011–1036.

Valera, J.-L., A.-M. Negredo, and A. Villaseñor (2008), Asymmetric delamination and convective removal numerical modeling: Comparison with evolutionary models for the Alboran Sea region, *Pure Appl. Geophys.*, *165*(8), 1683–1706, doi:10.1007/s00024-008-0395-8.

Vissers, R. L. M., J. P. Platt, and D. van der Wal (1995), Late orogenic extension of the Betic Cordillera and the Alboran Domain: A lithospheric view, *Tectonics*, *14*, 786–803, doi:10.1029/95TC00086.

Wortel, M. J. R., and W. Spakman (2000), Subduction and slab detachment in the Mediterranean-Carpathian Region, *Science*, *290*(5498), 1910–1917, doi:10.1126/science.290.5498.1910.

Zeck, H. P. (1996), Betic-Rif orogeny: Subduction of Mesozoic Tethys lithosphere under eastward drifting Iberia, slab detachment shortly before 22 Ma, and subsequent uplift and extensional tectonics, *Tectonophysics*, *254*(1–2), 1–16, doi:10.1016/0040-1951(95)00206-5.